



Article

The Influence of Composite Luminescent Materials Based on Graphene Oxide on the Growth and Development of *Solanum lycopersicum* in Greenhouses

Mark O. Pashkin ¹, Roman V. Pobedonostsev ¹, Dina V. Kazantseva ¹, Alexander V. Simakin ^{1,*}, Irina V. Gorudko ², Denis V. Yanykin ^{1,3} and Sergey V. Gudkov ^{1,4}

¹ Prokhorov General Physics Institute, Russian Academy of Sciences, Vavilov Str. 38, 119991 Moscow, Russia; pashin.mark@mail.ru (M.O.P.); pobedonoscevroman@rambler.ru (R.V.P.); dinacazantsewa@yandex.ru (D.V.K.); ya-d-ozh@rambler.ru (D.V.Y.); s_makariy@rambler.ru (S.V.G.)

² Department of Biophysics, Belarusian State University, 220006 Minsk, Belarus; irinagorudko@gmail.com

³ Institute of Basic Biological Problems, Russian Academy of Sciences, Federal Research Center “Pushchino Scientific Center for Biological Research” FRC PSCBR, Russian Academy of Sciences, 2 Institutskaya Str., 142290 Pushchino, Russia

⁴ Department of Biophysics, Lobachevsky State University, 23 Gagarin Avenue, 603950 Nizhny Novgorod, Russia

* Correspondence: avsimakin@gmail.com

Abstract: The effect of graphene oxide-based photoconversion covers on the growth and photosynthesis of tomatoes (*Solanum lycopersicum*) was investigated. Two types of photoconversion composite for covers were produced. In the first, only graphene oxide nanoparticles were used as a phosphor, and in the second, the graphene oxide nanoparticles were used jointly with europium oxide nanoparticles. The freshly prepared composites for covers had almost identical photoluminescence spectra: an intense peak in the red region and a minor peak in the blue region. It was revealed that during operation, luminescence in the red region decreased, while in the blue region it increased, probably due to the photothermal reduction of graphene oxide. It was shown that the photoconversion covers increased productivity (25%) and intensified photosynthesis (30–35%) in the tomato plants. It is suggested that the stimulation of plant growth is caused by changes in the light spectrum induced by the photoconversion covers.

Keywords: photoconversion; photoluminescence; graphene oxide; europium oxide; greenhouses; *Solanum lycopersicum*



Citation: Pashkin, M.O.; Pobedonostsev, R.V.; Kazantseva, D.V.; Simakin, A.V.; Gorudko, I.V.; Yanykin, D.V.; Gudkov, S.V. The Influence of Composite Luminescent Materials Based on Graphene Oxide on the Growth and Development of *Solanum lycopersicum* in Greenhouses. *J. Compos. Sci.* **2023**, *7*, 474. <https://doi.org/10.3390/jcs7110474>

Academic Editor: Francesco Tornabene

Received: 3 October 2023

Revised: 19 October 2023

Accepted: 2 November 2023

Published: 12 November 2023



Copyright: © 2023 by the authors. Licensee MDPI, Basel, Switzerland. This article is an open access article distributed under the terms and conditions of the Creative Commons Attribution (CC BY) license (<https://creativecommons.org/licenses/by/4.0/>).

1. Introduction

Light is an environmental factor whose characteristics have a strong influence on the growth and development of plants, as well as on their primary and secondary metabolisms [1–4]. The defining characteristics of light are the length of daylight hours and its spectral composition. Changes in daylight hours trigger changes in the phases of plant growth and development, and circadian rhythms. The spectrum of light is also of great importance for plants. Red light promotes plant photomorphogenesis, is critical for the development of the photosynthetic apparatus and the accumulation of sugars, and also regulates the synthesis of phytochemical compounds such as phenols [5]. Blue light regulates stomatal movement, the biosynthesis of chlorophyll and carotenoids, photomorphogenesis, as well as the synthesis of flavonoids and anthocyanins [6,7]. Supplemental illumination with green light under certain conditions can intensify photosynthesis in plants, and lead to an increase in the activity of enzymes of the antioxidant system and the accumulation of aromatic compounds in leaves [8]. Yellow light increases the isoflavonoid content in seedlings [9]. Thus, numerous studies have shown that, for the normal growth and development of plants, a careful selection of the lighting spectrum is necessary [10].

Currently, a variety of approaches are used to create optimal conditions for growing plants in greenhouses, from additional lighting in conditions of a lack of natural light to selective shading in conditions of excessive natural light. At the same time, the high cost of additional lighting reduces the profitability of production. Therefore, approaches aimed at changing the spectrum of sunlight are gaining great popularity [11–14]. Photosensitive [15–29] or photoconversion [30–33] coatings are used for these purposes. The first approach is based on reducing the intensity of the spectral component harmful to plants, or on changing the ratio of spectral components in order to influence the plant's receptor of regulatory systems. This approach allows researchers to increase plant productivity as well as create the definite phenotype. The second approach involves the selective absorption of light by phosphors and its re-emission in a different spectral range. This approach allows researchers, on the one hand, to increase PFD in a definite part of the spectrum and, on the other hand, to influence photoreceptors to trigger adaptive changes in the plant itself. At the present time, the light conversion approach is used not only for the acceleration of higher plant growth, but also for microalgae [34,35]. It has been shown that light-converting covers can be used for the regulation of the biomass and lipid productivity of microalgae. Currently, there are numerous phosphors on the market that are, more or less, suitable for creating photoconversion covers. Phosphors created on the basis of organic dyes have an undeniable advantage due to their low cost, ease of use, and high luminescence yield [36–45]; however, constant exposure to light leads to rapid irreversible photodegradation [46]. Another class of compounds are metal-containing nanoparticles [47–52]. Such phosphors have increased stability, but are more difficult to integrate into covers and have a low luminescence quantum yield [53–56]. To date, no photoconversion covers have been created that meet all requirements for greenhouse complexes. However, new materials with improved characteristics are regularly being created and tested.

A promising alternative to fast-degradation organic dyes and ineffective nanoparticles based on metal compounds may be the use of graphene oxide (GO) nanoluminophores. Due to its properties, graphene oxide has a wide range of applications: electronics, lithium-ion batteries, absorbents, catalysts (including photo- and electrocatalysis), etc. Currently, biocompatible materials have been obtained based on GO [57], which has opened opportunities for their application in biomedicine and tissue engineering. The luminescent properties of graphene oxide are of great interest. Unlike graphene, which is not capable of photoluminescence [58,59], GO-based materials are capable of photoluminescence in a wide range (350 nm–1250 nm), wherein the emission wavelength is determined by the degree of oxidation of graphene [58], which makes it possible to obtain graphene oxide with the determined photoluminescent properties. In this study, we tested the effectiveness of the application of graphene oxide as a phosphor in photoconversion covers for greenhouses. The study was performed using covers containing GO as the sole phosphor (PCC-GO) and GO with the addition of europium oxide composite (PPC-GO-Eu₂O₃).

2. Materials and Methods

2.1. Preparation of Nanoparticles and Study of Their Properties

GO nanoparticles were prepared via ultrasonic treatment of graphene oxide microparticles (prepared using the Hummers method (RusGraphene, Moscow, Russia)) during 1 min with a frequency of 40 kHz under room temperature. Eu₂O₃ nanoparticles were obtained via laser fragmentation of europium oxide powder (Sigma-Aldrich, Stockholm, Sweden, purity 99.99%) with laser (Ekspla, Vilnius, Lithuania), as described previously [60]. The hydrodynamic radius of the obtained nanoparticles was determined via dynamic light scattering using a Malvern Zetasizer ULTRA RED LABEL installation (Malvern panalytical Ltd., Worcestershire, UK) in an aqueous solution with scattering at 174.7° at 25 °C with tenfold measurements.

2.2. The Glass Surface Application of NF

A solution of nanoparticles in acetone (0.8 mg GO/mL and/or 0.6 µg Eu₂O₃/mL) was mixed with a liquid component of a fluoroplastic polymer (fluoroplastic-32L, St. Petersburg Paint and Varnish Plant, KRASKI SPB LLC, St. Petersburg, Russia) in a ratio of 1/ 100. The mixture was stirred for 10 min until homogeneous. The nanoparticles were applied to clean, grease-free glass using a spray gun with nozzle No. 4 from a distance of 20 cm and pressure of 2.5–3.0 atm. The consumption of the mixture was 33 mL per m² of surface. The covers applied to the glass were resistant to water and detergent solutions.

2.3. Fluorescence of PCC

Three-dimensional fluorescence spectra of the photoconversion covers were obtained using a Jasco FP-8300 Spectrofluorimeter (JASCO Applied Sciences, Victoria, BC, Canada) at room temperature.

2.4. Plant Growing Conditions

The work was carried out using the tomato plants (*Solanum lycopersicum*) determinate cultivar “Balkonnoe Chudo”. Seeds were planted in an organomineral plug moistened with nutrient solution as described earlier [60], which was placed under glass coated with a control (without phosphors) or the photoconversion cover. The nutrient solution contained 0.5 mM KNO₃; 0.67 mM Mg(NO₃)₂; 4.5 mM Ca(NO₃)₂; 2.2 mM K₂SO₄; 1 mM KH₂PO₄; and 2 mM MgSO₄. The illumination source was incandescent and UV lamps with a 16 h daylight period and a light intensity of ≈80 µmol photons s^{−1} m^{−2} at 25 °C.

2.5. Calculation of Chlorophyll Content in the Leaves of Plants

The chlorophyll content in the leaves was controlled non-invasively throughout the experiment using a CL-01 chlorophyll meter. To convert the records of the portable chlorophyll content meter to generally accepted units (mg chl × g^{−1} of fresh weight), the equation calculated for tomatoes was used [60].

2.6. Measuring the Kinetics of Photosynthetic Activity in the Plant Leaves

The photosynthetic activity in the plant leaves at 25 days after seed germination was determined by the kinetics of photoinduced changes in chlorophyll a fluorescence, the intensity of transpiration, and assimilation of carbon dioxide, using a DUAL-PAM-100 fluorimeter integrated with a GFS-3000 gas analyzer (Waltz, Eichenring, Effeltrich, Germany) at intensity active light 140 µmol photons s^{−1} m^{−2}, 50% humidity, CO₂ concentration of 200 ppm, and temperature of 25 °C. All measurements were performed in a closed chamber (L × W × H, 1 × 1 × 0.5 cm) and repeated at least three times. Fluorescence and gas exchange parameters were calculated with the DUAL-PAM (v.3.20) and GFS-win software (v.3.79), respectively [61–63].

2.7. Statistical Analysis

One-way analysis of variance (ANOVA) was performed to determine statistically significant differences between the plant groups, followed by post hoc comparisons using Student's *t* test for independent means. The difference was considered statistically significant if *p* ≤ 0.05.

3. Results

3.1. Properties of the Nanoparticles and the Photoconversion Covers

In this study, we used nanoparticles obtained by laser fragmentation of a colloid solution of europium oxide in deionized water. In the result of laser fragmentation, the colloid of nanoparticles, which formed aggregates, was prepared. It was shown that the size of the nanoparticles and their aggregates was 16 nm ± 5 nm and 200 nm ± 20 nm, respectively (Figure 1). The graphene oxide nanoparticles were 27 ± 5 nm (Figure 1). Then,

the nanoparticles were transferred from an aqueous solution into acetone, mixed with a fluoroplastic polymer (fluoroplastic-32L), and applied to the glass surface.

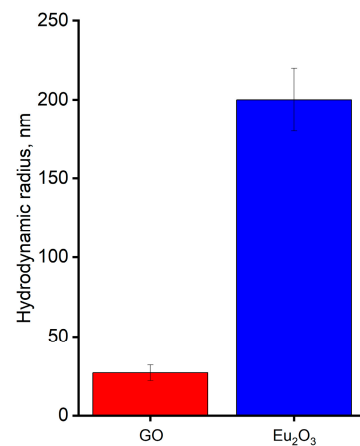


Figure 1. Weighted average particle hydrodynamic radius of GO (red column) and Eu₂O₃ (blue column) at a concentration of 0.8 mg GO/mL and 0.6 µg Eu₂O₃/mL. The measurements were performed in aqueous colloidal solutions of nanoparticles at 25 °C.

The differential (“spectrum of the photoconversion cover with luminophore composites + fluoroplastic 32L” minus “spectrum of common film with fluoroplastic 32L”) 3D luminescence matrix of the GO composite applied on the photoconversion cover was obtained before the experiment. It was revealed that the photoconversion cover is characterized by the presence of two luminescence peaks. The first peak is located in the red region ($540\text{ nm} < \lambda_{em} < 610\text{ nm}$) and the second peak is located in the blue region of the spectrum ($440\text{ nm} < \lambda_{em} < 490\text{ nm}$). The PCC luminescence in these ranges was induced by ultraviolet radiation up to 400 nm (Figure 2). The luminescence spectrum of PCC-GO-Eu₂O₃ was practically the same as for PCC-GO: the covers emitted in the blue (minor band) and red (major band) region under UV excitation. After an experiment with *S. lycopersicum*, we found that the intensity of red luminescence significantly decreased, and luminescence in the blue region, on the contrary, increased (Figure 3). This inversion of the luminescence maxima most likely occurred due to the photothermal reduction of graphene oxide [58].

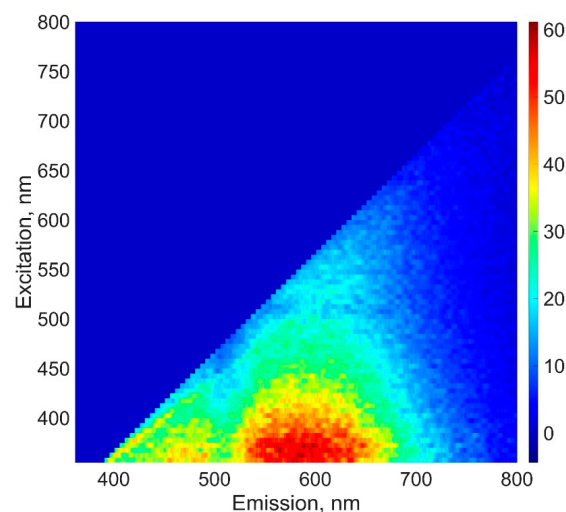


Figure 2. Three-dimensional fluorescence spectrum of the photoconversion cover with GO. The fluorescence intensity is expressed in arbitrary units using a color scale.

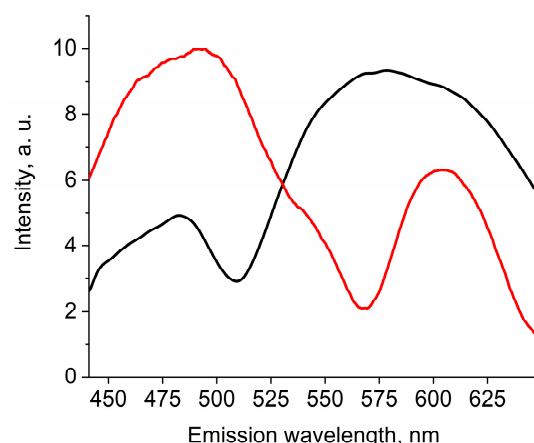


Figure 3. Fluorescence spectrum of the photoconversion cover with GO, excited at 375 nm before (A) and after (B) the experiment with the plants.

Further studies were aimed at testing the effect of the developed covers on the growth of *S. lycopersicum* in laboratory conditions under artificial light, simulating the lack of sunlight in protected soil conditions. The morphology, gas exchange, and photochemistry of the plants were studied.

3.2. Effect of the Photoconversion Covers on Plant Morphology

It was shown that the total leaf surface area was increased in the *S. lycopersicum* plants grown under PCCs by 26–37% in comparison to the control plants (Figure 4A) (without statistically significant differences between the PPC-GO and PPC-GO-Eu₂O₃ plants). PCCs also increased the number of leaves by 8–15% (Figure 4B). However, PCCs did not affect the length of internodes, the ratio of the leaf fresh weight to dry weight, or the chlorophyll content (Figure 4C) in the studied plants. Thus, the obtained data indicate that the developed graphene oxide-based composites applied on the glass surface have a stimulation effect on the growth of the tomato plants.

3.3. Effect of the Photoconversion Covers on the Gas Exchange Parameters in the Plants

Figure 5 shows the kinetics of light-induced changes in transpiration rates, CO₂ assimilation, and water use efficiency in the *S. lycopersicum* leaves (Figure 5A–C). In the dark, there was no uptake of CO₂ by the tomato leaves, but its release was observed at 0.23 μmol CO₂/m² s–0.25 μmol CO₂/m² s, without statistically significant differences between the studied groups of plants. This effect was associated with light-independent processes in the leaf tissues, for example, cellular respiration, and processes of the Calvin cycle (Figure 5A). Turning on the light activated CO₂ assimilation in all studied groups of tomato plants, which usually occurs in three phases: (1) a rapid increase in the intensity of CO₂ assimilation in the first minutes of the lighting, associated with the consumption of the reserve of ribulose-1,5-bisphosphate or other intermediate products of the Calvin cycle; (2) a slow growth for 7–10 min of the lighting, when photoactivation of Rubisco by Rubisco activase occurs; and (3) a stationary phase, observed when the maximum intensity of CO₂ assimilation is achieved. The figure shows that during light irradiation of the control plants, the phase of rapid growth of CO₂ assimilation intensity was not observed, while in the plants grown under the experimental covers, the assimilation CO₂ intensity in this phase reaches 1.4 μmol CO₂/m² s–1.5 μmol CO₂/m² s. The growth rate of CO₂ assimilation intensity in the second phase was similar for all groups of plants. These data may indicate different amounts of Calvin cycle intermediates in the control and experimental plants. At the stationary phase, the maximum intensity of assimilation rate was 25% higher in the plants that were grown under the experimental covers with graphene oxide composites (2.84 μmol CO₂/m² s) than in the control plants (2.12 μmol CO₂/m² s), probably due to the fact that during the measurement, the intensity of CO₂ assimilation did not manage to reach

maximum values. The intensity of transpiration of H_2O in the dark was the same for all groups of plants, namely, $0.13 \text{ mmol } H_2O/m^2 \text{ s}$ – $0.23 \text{ mmol } H_2O/m^2 \text{ s}$, without statistically significant differences between the studied groups of plants. Turning on the light activated the transpiration of H_2O in the leaves of all plant groups (Figure 5B). However, in the plants grown under the developed photoconversion covers, the activation of transpiration occurs almost immediately, whereas in the control plants, activation begins only after five minutes. The intensity of transpiration at the end of the lighting period was the same in all groups of plants, namely, $0.56 \text{ mmol } H_2O/m^2 \text{ s}$ – $0.76 \text{ mmol } H_2O/m^2 \text{ s}$. Differences in water use efficiency between the control and the experimental plants were observed only in the first minutes of illumination, and are more likely due to the lack of a “fast” assimilation growth phase in the plants grown under control covers (Figure 5C). Figure 5 shows that the changes in transpiration and assimilation rates induced by continuous illumination are accompanied by periodic disturbances. These disturbances arise due to the switching on, every minute, of a saturating flash generated by a PAM-fluorometer operating in tandem with a gas analyzer. Despite the fact that the analysis of flash-induced changes in these parameters was not part of the objectives of this study, we noted that the amplitude of such oscillations was higher in plants grown under PCCs.

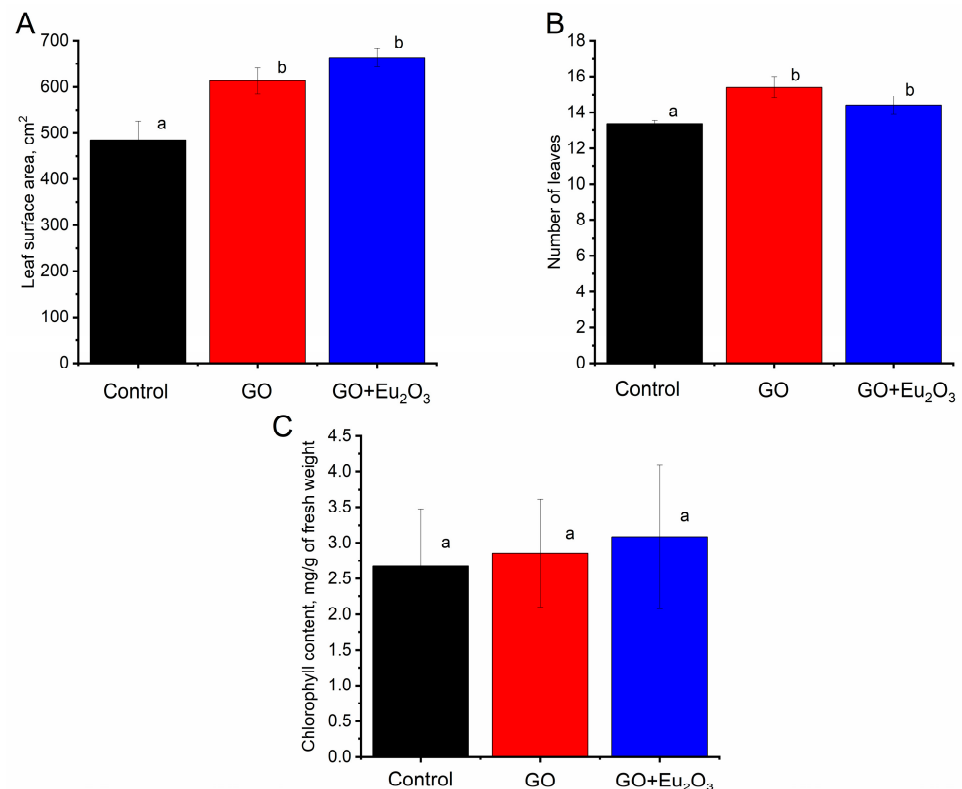


Figure 4. The effect of the photoconversion covers on the leaf surface area (A), number of leaves (B), chlorophyll content (C) of *S. lycopersicum*, measured on the thirty-eighth day after seeding. The data are the result of averaging nine measurements. The letters a, b indicate statistically significant differences between the plant groups ($p \leq 0.05$). PCC-GO are the plants growing under covers containing GO as the sole phosphor, and PPC-GO-Eu₂O₃ are the plants growing under covers with the addition of GO and europium oxide.

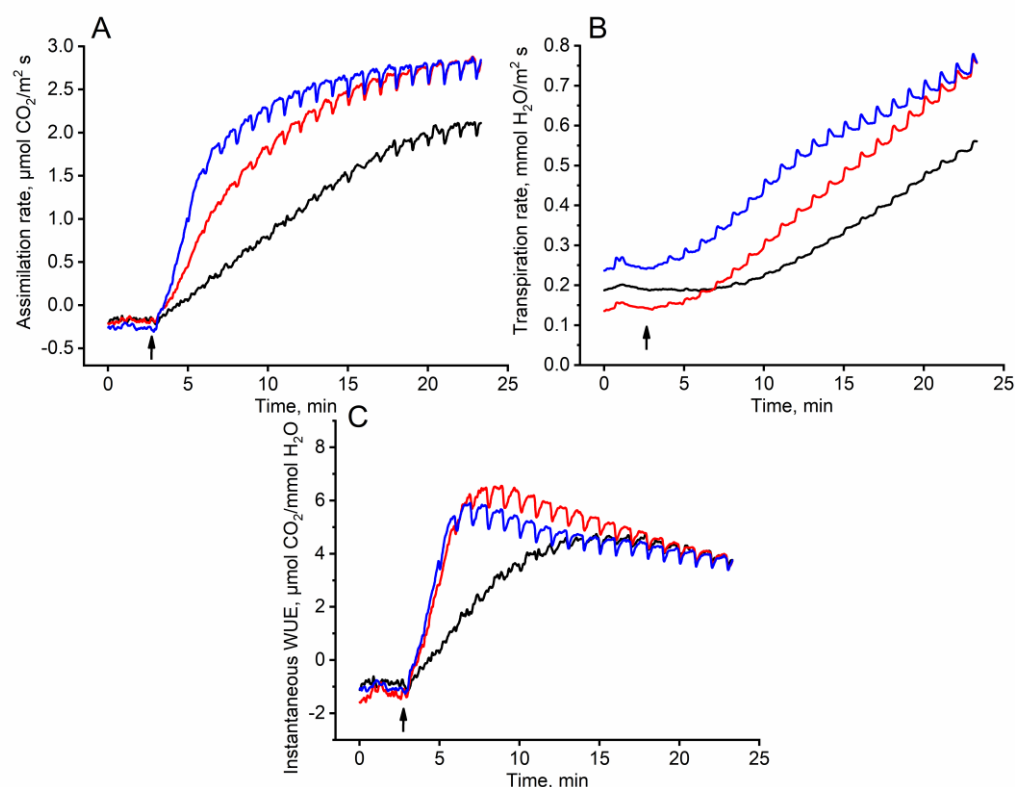


Figure 5. Kinetics of light-induced changes in the intensity of CO₂ assimilation (A), transpiration (B), and instantaneous water use efficiency (C) in the leaves of *S. lycopersicum*. The measurements were performed using plants growing under control covers (black curve), plants growing under PCC-GO (red curve), and plants growing under PCC-GO-Eu₂O₃ (blue curve) at 25 °C, 50% humidity and CO₂ concentration of 200 ppm. ↑—the moment of turning on the acting light ($\lambda = 625 \text{ nm}$, $140 \mu\text{mol photons m}^{-2} \text{ s}^{-1}$). All plants were dark-adapted for 1 h.

3.4. Effect of the Photoconversion Covers on Plant Photochemistry

Further work was devoted to the registration of photoinduced changes in chlorophyll a fluorescence, representing the efficiency of electron transfer in the photosynthetic electron transport chain and related processes. It was revealed that the maximum quantum yield of the photosystem II photochemistry (F_v/F_m) in all groups of plants was the same, namely, 0.80–0.81, without statistically significant differences between the studied groups of plants. However, other parameters of chlorophyll fluorescence were different in the experimental and control groups of plants (Figure 6). The plants grown under the experimental PCCs had increased the effective quantum yield of photosystem II ($Y(II)$) by 28–36%. Statistically significant differences between the plants grown under PCC-GO and PCC-GO-Eu₂O₃ were not observed (Figure 6A). The PCCs also increased the electron transport rate of photosystem II ($ETR(II)$) by 26–35%, without statistically significant differences between the experimental groups of plants (Figure 6B). These changes can indicate a more intense dark stage of photosynthesis in experimental plants. The effective quantum yield of the photosystem I ($Y(I)$) value in the leaves of the experimental plants differed from that in the control plants only in the first few minutes after turning on the light; then, the differences gradually decreased and disappeared after ten minutes of illumination (Figure 6C). Statistically significant differences between the plants grown under PCC-GO and PCC-GO-Eu₂O₃ were not observed during the illumination. The quantum yield of nonphotochemical quenching of chlorophyll a fluorescence ($Y(NPQ)$) in the control plants, in contrast to $Y(II)$ and $ETR(II)$, was higher than in the plants grown under PCCs, without statistically significant differences between the two groups (Figure 6D).

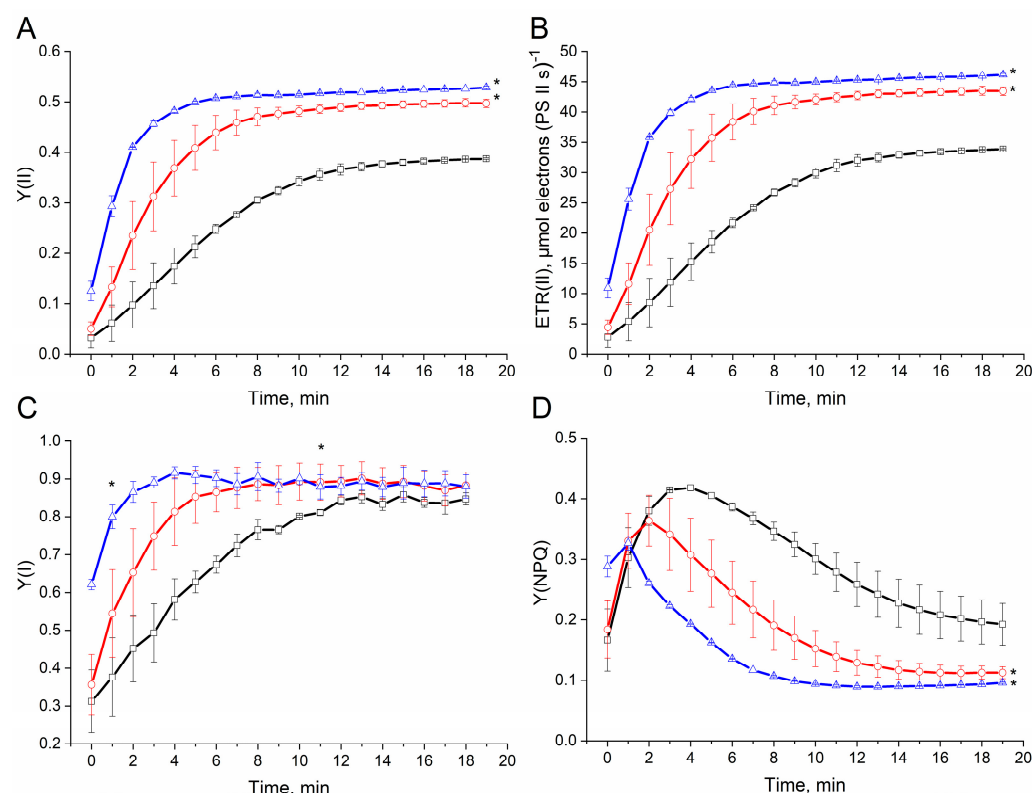


Figure 6. Light-induced changes in the parameters of the effective quantum yield of PSII (A), the rate of linear electron transport per PSII reaction center (B), the effective quantum yield of PSI (C), and the quantum yield of light-induced non-photochemical quenching of chlorophyll a fluorescence (D) in the leaves of *S. lycopersicum*. The measurements were performed using plants growing under control covers (black curve), plants growing under PCC-GO (red curve), and plants growing under PCC-GO-Eu₂O₃ (blue curve). Before the measurements, the plants were adapted in the dark for 1 h at 25 °C. The intensity of the 300 ms saturating light pulses was 12,000 $\mu\text{mol photons m}^{-2} \text{s}^{-1}$. * denotes statistically significant differences between the experimental and control plant groups ($p \leq 0.05$).

Thus, the present data indicate that an intensification of photosynthesis in the plants grown under the PCCs led to an increase in plant growth.

4. Discussion

Graphene oxide consists of graphene particles modified at the edges or inside the carbon network with oxygen-containing functional groups in the form of epoxy, hydroxyl, phenolic, carboxyl, ether, and other groups [64]. The mass fraction of oxygen atoms in the GO can vary from 3% to 40%. GO is effectively used in many fields of science, from biomedicine to energy [65–69], as well as in agriculture [70–76]. It is important that nanosized GO particles have now been obtained that are highly biocompatible with mammalian and plant cells [77–80]. At the same time, studies on the influence of GO on plants have focused on the response of the plants to the addition of graphene oxide along with a nutrient solution or when sprayed.

Graphene oxides have very diverse fluorescent properties [81–88]. Depending on the conditions, pre-treatments, and synthesis method, GO can fluoresce in the red and infrared regions (typical of suspensions of freshly synthesized GO particles), in the entire visible range of the spectrum (graphene sheet after treatment with oxygen plasma), or in the blue region (after exposure to ultraviolet light, chemical reducing agents, or thermal annealing in an inert environment), wherein the quantum yield varies on average from 4% to 30% [89–93].

The nanosized GO in our study has intense luminescence in the red and weak luminescence in the blue part of the spectrum, which allowed us to study the effect of

photoconversion covers based on graphene oxide on the growth and photosynthetic activity of tomato plants. Unfortunately, we were unable to find other examples of the application of graphene oxide to create photoconversion covers for greenhouses. This may be the first time this has been done in research.

The effect of the inversion of the luminescence maxima of the photoconversion covers can be explained by the effect of the photothermal reduction of graphene oxide. It was previously shown that the illumination of GO with a xenon lamp leads to an increase in the proportion of carbon atoms linked by sp^2 bonds ($C=C$) as a result of deoxygenation from 25% to 69% for 3 h, which is accompanied by a shift of the luminescence maximum from the red to the blue region of the spectrum [58]. Thus, we have shown that in the first days of the experiment, the luminescent properties of covers based on graphene oxide were unstable. On the 25th day of the experiment, the short-wavelength luminescence (about 450 nm) increased and the red peak decreased, as a result of which the graphene oxide in the covers became a blue phosphor (Figure 3).

It is known that graphene oxide nanoparticles tend to aggregate and assemble into sheets, wherein the addition of various nanoparticles, including lanthanide oxides such as europium oxide, prevents agglomeration [94]. Thus, we hypothesized that europium oxide nanoparticles could improve the photoconversion properties of the developed graphene oxide-based covers both by improving the structural properties of graphene oxide nanoparticles and adding luminophores, which was effective in the photoconversion cover [60]. However, our assumption was not confirmed, because there were no significant changes in the morphology, physiology, and photochemistry of the tomatoes (Figures 4–6). We also noted that the addition of the Eu_2O_3 nanoparticles to a colloid containing GO nanoparticles practically does not change the luminescent properties of the colloid. Probably, when mixed, GO nanoparticles are adsorbed on the aggregates of the Eu_2O_3 nanoparticles, preventing the excitation and quenching the luminescence of the latter. Previously, in studies on the adsorption of europium ions on graphene oxide, it was found that $Eu(III)$ interacts with the carbonyl, carboxyl, epoxy, and alkoxy groups of graphene oxide [95–97].

The increased solar energy absorption efficiency observed in the tomato plants grown under PCC-GO and PCC-GO Eu_2O_3 (Figure 6) leads to an increased CO_2 assimilation (Figure 5A), which ultimately increases plant productivity (Figure 4). The result obtained may be due to several changes in the lighting spectrum at once. Firstly, the photoconversion covers effectively absorb ultraviolet radiation, which can have a harmful effect on the plants [98,99]. On the other hand, a decrease in UV intensity is accompanied by an increase in PAR intensity (in the red or blue regions at the beginning or end of the experiment, respectively). It is known that plants exhibit maximum photosynthetic activity in red and blue light, and it is red and blue light that most effectively stimulate photosynthesis under low light conditions [100]. Red and blue light are involved in regulating the opening of stomata, thereby increasing the intensity of CO_2 assimilation. However, the exact mechanism of the stomatal movement in response to the red light is still unknown. An increase in the amount of red light can lead to a change in the red light/far-red light ratio and subsequently affect the functioning of the phytochrome system, which can regulate plant growth and influence its resistance when exposed to stress factors [101].

Thus, photoconversion covers based on graphene oxide as a phosphor were created, which have a positive effect on plant growth and photosynthesis. It was revealed that during the experiment, graphene oxide nanoparticles undergo modifications, turning from red to blue, without losing their efficiency.

Author Contributions: Conceptualization, A.V.S. and S.V.G.; methodology, A.V.S., S.V.G. and D.V.Y.; investigation, D.V.Y., M.O.P., R.V.P., I.V.G. and D.V.K.; writing—original draft preparation, M.O.P. and D.V.Y.; writing—review and editing, D.V.Y. and S.V.G.; visualization, M.O.P.; funding acquisition, S.V.G. All authors have read and agreed to the published version of the manuscript.

Funding: This work was supported by a grant from the Ministry of Science and Higher Education of the Russian Federation (075-15-2022-315) for the organization and development of the world-class research center “Photonics”.

Data Availability Statement: The data presented in this study are available on request from the corresponding author.

Conflicts of Interest: The authors declare no conflict of interest.

References

1. Arena, C.; Tsonev, T.; Doneva, D.; De Micco, V.; Michelozzi, M.; Brunetti, C.; Centritto, M.; Fineschi, S.; Velikova, V.; Loreto, F. The Effect of Light Quality on Growth, Photosynthesis, Leaf Anatomy and Volatile Isoprenoids of a Monoterpene-Emitting Herbaceous Species (*Solanum lycopersicum* L.) and an Isoprene-Emitting Tree (*Platanus orientalis* L.). *Environ. Exp. Bot.* **2016**, *130*, 122–132. [\[CrossRef\]](#)
2. Miao, L.; Zhang, Y.; Yang, X.; Xiao, J.; Zhang, H.; Zhang, Z.; Wang, Y.; Jiang, G. Colored Light-Quality Selective Plastic Films Affect Anthocyanin Content, Enzyme Activities, and the Expression of Flavonoid Genes in Strawberry (*Fragaria × ananassa*) Fruit. *Food Chem.* **2016**, *207*, 93–100. [\[CrossRef\]](#) [\[PubMed\]](#)
3. Astashev, M.E.; Serov, D.A.; Gudkov, S.V. Application of Spectral Methods of Analysis for Description of Ultradian Biorhythms at the Levels of Physiological Systems, Cells and Molecules (Review). *Mathematics* **2023**, *11*, 3307. [\[CrossRef\]](#)
4. Esmaeilzadeh, M.; Shamsabad, M.R.M.; Roosta, H.R.; Dabrowski, P.; Rapacz, M.; Zielinski, A.; Wrobel, J.; Kalaji, H.M. Manipulation of Light Spectrum Can Improve the Performance of Photosynthetic Apparatus of Strawberry Plants Growing under Salt and Alkalinity Stress. *PLoS ONE* **2021**, *16*, e0261585. [\[CrossRef\]](#) [\[PubMed\]](#)
5. Lee, S.W.; Seo, J.M.; Lee, M.K.; Chun, J.H.; Antonisamy, P.; Arasu, M.V.; Suzuki, T.; Al-Dhabi, N.A.; Kim, S.J. Influence of Different LED Lamps on the Production of Phenolic Compounds in Common and Tartary Buckwheat Sprouts. *Ind. Crops Prod.* **2014**, *54*, 320–326. [\[CrossRef\]](#)
6. Xu, F.; Cao, S.; Shi, L.; Chen, W.; Su, X.; Yang, Z. Blue Light Irradiation Affects Anthocyanin Content and Enzyme Activities Involved in Postharvest Strawberry Fruit. *J. Agric. Food Chem.* **2014**, *62*, 4778–4783. [\[CrossRef\]](#)
7. Chen, X.L.; Yang, Q.C.; Song, W.P.; Wang, L.C.; Guo, W.Z.; Xue, X.Z. Growth and Nutritional Properties of Lettuce Affected by Different Alternating Intervals of Red and Blue LED Irradiation. *Sci. Hortic.* **2017**, *223*, 44–52. [\[CrossRef\]](#)
8. Bian, Z.; Yang, Q.; Li, T.; Cheng, R.; Barnett, Y.; Lu, C. Study of the Beneficial Effects of Green Light on Lettuce Grown under Short-Term Continuous Red and Blue Light-Emitting Diodes. *Physiol. Plant* **2018**, *164*, 226–240. [\[CrossRef\]](#)
9. Lee, S.J.; Ahn, J.K.; Khanh, T.D.; Chun, S.C.; Kim, S.L.; Ro, H.M.; Song, H.K.; Chung, I.M. Comparison of Isoflavone Concentrations in Soybean (*Glycine max* (L.) Merrill) Sprouts Grown under Two Different Light Conditions. *J. Agric. Food Chem.* **2007**, *55*, 9415–9421. [\[CrossRef\]](#)
10. Wang, J.; Lu, W.; Tong, Y.; Yang, Q. Leaf Morphology, Photosynthetic Performance, Chlorophyll Fluorescence, Stomatal Development of Lettuce (*Lactuca sativa* L.) Exposed to Different Ratios of Red Light to Blue Light. *Front. Plant Sci.* **2016**, *7*, 176122. [\[CrossRef\]](#)
11. Smirnov, A.A.; Semenova, N.A.; Dorokhov, A.S.; Proshkin, Y.A.; Godyaeva, M.M.; Vodeneev, V.; Sukhov, V.; Panchenko, V.; Chilingaryan, N.O. Influence of Pulsed, Scanning and Constant (16- and 24-h) Modes of LED Irradiation on the Physiological, Biochemical and Morphometric Parameters of Lettuce Plants (*Lactuca sativa* L.) While Cultivated in Vertical Farms. *Agriculture* **2022**, *12*, 1988. [\[CrossRef\]](#)
12. Semenova, N.A.; Smirnov, A.A.; Dorokhov, A.S.; Proshkin, Y.A.; Ivanitskikh, A.S.; Chilingaryan, N.O.; Dorokhov, A.A.; Yanykin, D.V.; Gudkov, S.V.; Izmailov, A.Y. Evaluation of the Effectiveness of Different LED Irradiators When Growing Red Mustard (*Brassica juncea* L.) in Indoor Farming. *Energies* **2022**, *15*, 8076. [\[CrossRef\]](#)
13. Semenova, N.A.; Smirnov, A.A.; Ivanitskikh, A.S.; Izmailov, A.Y.; Dorokhov, A.S.; Proshkin, Y.A.; Yanykin, D.V.; Sarimov, R.R.; Gudkov, S.V.; Chilingaryan, N.O. Impact of Ultraviolet Radiation on the Pigment Content and Essential Oil Accumulation in Sweet Basil (*Ocimum basilicum* L.). *Appl. Sci.* **2022**, *12*, 7190. [\[CrossRef\]](#)
14. Tikhonov, P.; Morenko, K.; Sycho, A.; Bolshev, V.; Sokolov, A.; Smirnov, A. LED Lighting Agrosystem with Parallel Power Supply from Photovoltaic Modules and a Power Grid. *Agriculture* **2022**, *12*, 1215. [\[CrossRef\]](#)
15. Wilson, S.B.; Rajapakse, N.C. Growth Control of Lisianthus by Photoselective Plastic Films. *Horttechnology* **2001**, *11*, 581–584. [\[CrossRef\]](#)
16. Doukas, D.; Payne, C.C. The Use of Ultraviolet-Blocking Films in Insect Pest Management in the UK; Effects on Naturally Occurring Arthropod Pest and Natural Enemy Populations in a Protected Cucumber Crop. *Ann. Appl. Biol.* **2007**, *151*, 221–231. [\[CrossRef\]](#)
17. García-Macías, P.; Ordidge, M.; Vysini, E.; Waroonphan, S.; Battey, N.H.; Gordon, M.H.; Hadley, P.; John, P.; Lovegrove, J.A.; Wagstaffe, A. Changes in the Flavonoid and Phenolic Acid Contents and Antioxidant Activity of Red Leaf Lettuce (Lollo rosso) Due to Cultivation under Plastic Films Varying in Ultraviolet Transparency. *J. Agric. Food Chem.* **2007**, *55*, 10168–10172. [\[CrossRef\]](#) [\[PubMed\]](#)
18. Kittas, C.; Tchamitchian, M.; Katsoulas, N.; Karaiskou, P.; Papaioannou, C. Effect of Two UV-Absorbing Greenhouse-Covering Films on Growth and Yield of an Eggplant Soilless Crop. *Sci. Hortic.* **2006**, *110*, 30–37. [\[CrossRef\]](#)

19. Lamnatou, C.; Chemisana, D. Solar Radiation Manipulations and Their Role in Greenhouse Claddings: Fresnel Lenses, NIR- and UV-Blocking Materials. *Renew. Sustain. Energy Rev.* **2013**, *18*, 271–287. [\[CrossRef\]](#)
20. Wilson, S.B.; Rajapakse, N.C. Growth Regulation of Sub-Tropical Perennials by Photosensitive Plastic Films. *J. Environ. Hortic.* **2001**, *19*, 65–68. [\[CrossRef\]](#)
21. Cerny, T.A.; Faust, J.E.; Layne, D.R.; Rajapakse, N.C. Influence of Photosensitive Films and Growing Season on Stem Growth and Flowering of Six Plant Species. *J. Am. Soc. Hortic. Sci.* **2003**, *128*, 486–491. [\[CrossRef\]](#)
22. Fletcher, J.M.; Tatsiopoulou, A.; Mpezamihigo, M.; Carew, J.G.; Henbest, R.G.C.; Hadley, P. Far-Red Light Filtering by Plastic Film, Greenhouse-Cladding Materials: Effects on Growth and Flowering in Petunia and Impatiens. *J. Hortic. Sci. Biotechnol.* **2005**, *80*, 303–306. [\[CrossRef\]](#)
23. Kambalapally, V.R.; Rajapakse, N.C. Spectral Filters Affect Growth, Flowering, and Postharvest Quality of Easter Lilies. *HortScience* **1998**, *33*, 1028–1029. [\[CrossRef\]](#)
24. Hebert, D.; Boonekamp, J.; Parrish, C.H.; Ramasamy, K.; Makarov, N.S.; Castañeda, C.; Schuddebeurs, L.; McDaniel, H.; Bergren, M.R. Luminescent Quantum Dot Films Improve Light Use Efficiency and Crop Quality in Greenhouse Horticulture. *Front. Chem.* **2022**, *10*, 988227. [\[CrossRef\]](#) [\[PubMed\]](#)
25. Rajapakse, N.C.; Kelly, J.W. Regulation of Chrysanthemum Growth by Spectral Filters. *J. Am. Soc. Hortic. Sci.* **1992**, *117*, 481–485. [\[CrossRef\]](#)
26. Rajapakse, N.C.; Kelly, J.W. Influence of Spectral Filters on Growth and Postharvest Quality of Potted Miniature Roses. *Sci. Hortic.* **1994**, *56*, 245–255. [\[CrossRef\]](#)
27. Causin, H.F.; Jauregui, R.N.; Barneix, A.J. The Effect of Light Spectral Quality on Leaf Senescence and Oxidative Stress in Wheat. *Plant Sci.* **2006**, *171*, 24–33. [\[CrossRef\]](#)
28. Noë, N.; Eccher, T.; Del Signore, E.; Montoldi, A. Growth and Proliferation in Vitro of Vaccinium Corymbosum under Different Irradiance and Radiation Spectral Composition. *Biol. Plant* **1998**, *41*, 161–167. [\[CrossRef\]](#)
29. Stagnari, F.; Galieni, A.; Cafiero, G.; Pisante, M. Application of Photo-Selective Films to Manipulate Wavelength of Transmitted Radiation and Photosynthate Composition in Red Beet (*Beta vulgaris* var. conditiva Alef.). *J. Sci. Food Agric.* **2014**, *94*, 713–720. [\[CrossRef\]](#)
30. Shen, L.; Yin, X. Solar Spectral Management for Natural Photosynthesis: From Photonics Designs to Potential Applications. *Nano Converg.* **2022**, *9*, 1–16. [\[CrossRef\]](#)
31. Wondraczek, L.; Tyystjärvi, E.; Méndez-Ramos, J.; Müller, F.A.; Zhang Wondraczek, Q.L.; Müller Otto Schott, F.A.; Wondraczek, L.; Müller, F.A.; Tyystjärvi, E.; Méndez-Ramos, J.; et al. Shifting the Sun: Solar Spectral Conversion and Extrinsic Sensitization in Natural and Artificial Photosynthesis. *Adv. Sci.* **2015**, *2*, 1500218. [\[CrossRef\]](#) [\[PubMed\]](#)
32. Ooms, M.D.; Dinh, C.T.; Sargent, E.H.; Sinton, D. Photon Management for Augmented Photosynthesis. *Nat. Commun.* **2016**, *7*, 1–13. [\[CrossRef\]](#)
33. Pashkin, M.O.; Yanykin, D.V.; Gudkov, S.V. Current Approaches to Light Conversion for Controlled Environment Agricultural Applications: A Review. *Horticultrae* **2022**, *8*, 885. [\[CrossRef\]](#)
34. Hwang, T.G.; Kim, G.-Y.; Han, J.-I.; Park, J.M.; Kim, J.P. Highly efficient light-converting films based on diketopyrrolopyrrole with deep-red aggregation-induced emission for enhancing the lipid productivity of *Chlorella* sp. *Sustain. Energy Fuels* **2021**, *5*, 5205–5215. [\[CrossRef\]](#)
35. Hwang, T.G.; Kim, G.-Y.; Han, J.-I.; Kim, S.; Kim, J.P. Enhancement of Lipid Productivity of *Chlorella* sp. Using Light-Converting Red Fluorescent Films Based on Aggregation-Induced Emission. *ACS Sustain. Chem. Eng.* **2020**, *8*, 15888–15897. [\[CrossRef\]](#)
36. Winsel, M. Light Manipulating Additives Extend Opportunities for Agricultural Plastic Films. *Plast. Addit. Compd.* **2002**, *4*, 20–24. [\[CrossRef\]](#)
37. Hamada, K.; Shimasaki, K.; Ogata, T.; Nishimura, Y.; Nakamura, K.; Oyama-Egawa, H.; Yoshida, K. Effects of Spectral Composition Conversion Film and Plant Growth Regulators on Proliferation of Cymbidium Protocorm Like Body (PLB) Cultured In Vitro. *Environ. Control. Biol.* **2010**, *48*, 127–132. [\[CrossRef\]](#)
38. Hemming, S.; van Os, E.A.; Hemming, J.; Dieleman, J.A. The Effect of New Developed Fluorescent Greenhouse Films on the Growth of *Fragaria x ananassa* “Elsanta”. *Eur. J. Hortic. Sci.* **2006**, *71*, 145–154.
39. Hidaka, K.; Yoshida, K.; Shimasaki, K.; Murakami, K.; Yasutake, D.; Kitano, M. Spectrum Conversion Film for Regulation of Plant Growth. *J. Fac. Agric. Kyushu Univ.* **2008**, *53*, 549–552. [\[CrossRef\]](#)
40. Kang, J.H.; Yoon, H.I.; Lee, J.M.; Kim, J.P.; Son, J.E. Electron Transport and Photosynthetic Performance in *Fragaria x Ananassa* Duch. Acclimated to the Solar Spectrum Modified by a Spectrum Conversion Film. *Photosynth. Res.* **2021**, *151*, 31–46. [\[CrossRef\]](#)
41. Novoplansky, A.; Sachs, T.; Cohen, D.; Bar, R.; Bodenheimer, J.; Reisfeld, R. Increasing Plant Productivity by Changing the Solar Spectrum. *Sol. Energy Mater.* **1990**, *21*, 17–23. [\[CrossRef\]](#)
42. Sánchez-Lanuz, M.B.; Menéndez-Velázquez, A.; Peñas-Sanjuan, A.; Navas-Martos, F.J.; Lillo-Bravo, I.; Delgado-Sánchez, J.M. Advanced Photonic Thin Films for Solar Irradiation Tuneability Oriented to Greenhouse Applications. *Materials* **2021**, *14*, 2357. [\[CrossRef\]](#) [\[PubMed\]](#)
43. Schettini, E.; de Salvador, F.R.; Scarascia-Mugnozza, G.; Vox, G. Radiometric Properties of Photosensitive and Photoluminescent Greenhouse Plastic Films and Their Effects on Peach and Cherry Tree Growth. *J. Hortic. Sci. Biotechnol.* **2011**, *86*, 79–83. [\[CrossRef\]](#)
44. Yalçın, R.A.; Ertürk, H. Improving Crop Production in Solar Illuminated Vertical Farms Using Fluorescence Coatings. *Biosyst. Eng.* **2020**, *193*, 25–36. [\[CrossRef\]](#)

45. Makarov, N.S.; Ramasamy, K.; Jackson, A.; Velarde, A.; Castaneda, C.; Archuleta, N.; Hebert, D.; Bergren, M.R.; McDaniel, H. Fiber-Coupled Luminescent Concentrators for Medical Diagnostics, Agriculture, and Telecommunications. *ACS Nano* **2019**, *13*, 9112–9121. [\[CrossRef\]](#)
46. Chiu, Y.H.; Chang, T.F.M.; Chen, C.Y.; Sone, M.; Hsu, Y.J. Mechanistic Insights into Photodegradation of Organic Dyes Using Heterostructure Photocatalysts. *Catalysts* **2019**, *9*, 430. [\[CrossRef\]](#)
47. Gudkov, S.V.; Simakin, A.V.; Bunkin, N.F.; Shafeev, G.A.; Astashev, M.E.; Glinushkin, A.P.; Grinberg, M.A.; Vodeneev, V.A. Development and Application of Photoconversion Fluoropolymer Films for Greenhouses Located at High or Polar Latitudes. *J. Photochem. Photobiol. B* **2020**, *213*, 112056. [\[CrossRef\]](#)
48. Simakin, A.V.; Ivanyuk, V.V.; Dorokhov, A.S.; Gudkov, S.V. Photoconversion Fluoropolymer Films for the Cultivation of Agricultural Plants Under Conditions of Insufficient Insolation. *Appl. Sci.* **2020**, *10*, 8025. [\[CrossRef\]](#)
49. Wu, W.; Zhang, Z.; Dong, R.; Xie, G.; Zhou, J.; Wu, K.; Zhang, H.; Cai, Q.; Lei, B. Characterization and Properties of a Sr₂Si₅N₈:Eu²⁺-Based Light-Conversion Agricultural Film. *J. Rare Earths* **2020**, *38*, 539–545. [\[CrossRef\]](#)
50. Parrish, C.H.; Hebert, D.; Jackson, A.; Ramasamy, K.; McDaniel, H.; Giacomelli, G.A.; Bergren, M.R. Optimizing Spectral Quality with Quantum Dots to Enhance Crop Yield in Controlled Environments. *Commun. Biol.* **2021**, *4*, 1–9. [\[CrossRef\]](#)
51. Ivanyuk, V.V.; Shkirin, A.V.; Belosludtsev, K.N.; Dubinin, M.V.; Kozlov, V.A.; Bunkin, N.F.; Dorokhov, A.S.; Gudkov, S.V. Influence of Fluoropolymer Film Modified with Nanoscale Photoluminophor on Growth and Development of Plants. *Front. Phys.* **2020**, *8*, 1–6. [\[CrossRef\]](#)
52. Pogreb, R.; Finkelshtein, B.; Shmukler, Y.; Musina, A.; Popov, O.; Stanevsky, O.; Yitzchaik, S.; Gladkikh, A.; Schulzinger, A.; Streltsov, V.; et al. Low-Density Polyethylene Films Doped with Europium(III) Complex: Their Properties and Applications. *Polym. Adv. Technol.* **2004**, *15*, 414–418. [\[CrossRef\]](#)
53. Ziessel, R.; Diring, S.; Kadjane, P.; Charbonnière, L.; Retaillieu, P.; Philouze, C. Highly Efficient Blue Photoexcitation of Europium in a Bimetallic Pt–Eu Complex. *Chem. Asian J.* **2007**, *2*, 975–982. [\[CrossRef\]](#) [\[PubMed\]](#)
54. Fitzmorris, B.C.; Pu, Y.C.; Cooper, J.K.; Lin, Y.F.; Hsu, Y.J.; Li, Y.; Zhang, J.Z. Optical Properties and Exciton Dynamics of Alloyed Core/Shell/Shell Cd 1–xZnxSe/ZnSe/ZnS Quantum Dots. *ACS Appl. Mater. Interfaces* **2013**, *5*, 2893–2900. [\[CrossRef\]](#)
55. Nguyen, A.T.; Lin, W.H.; Lu, Y.H.; Chiou, Y.D.; Hsu, Y.J. First Demonstration of Rainbow Photocatalysts Using Ternary Cd_{1–x}ZnxSe Nanorods of Varying Compositions. *Appl. Catal. A Gen.* **2014**, *476*, 140–147. [\[CrossRef\]](#)
56. Pu, Y.C.; Chen, W.T.; Fang, M.J.; Chen, Y.L.; Tsai, K.A.; Lin, W.H.; Hsu, Y.J. Au–Cd_{1–x}ZnxS Core–Alloyed Shell Nanocrystals: Boosting the Interfacial Charge Dynamics by Adjusting the Shell Composition. *J. Mater. Chem. A Mater.* **2018**, *6*, 17503–17513. [\[CrossRef\]](#)
57. Yadav, S.; Singh Raman, A.P.; Meena, H.; Goswami, A.G.; Bhawna; Kumar, V.; Jain, P.; Kumar, G.; Sagar, M.; Rana, D.K.; et al. An Update on Graphene Oxide: Applications and Toxicity. *ACS Omega* **2022**, *7*, 35387–35445. [\[CrossRef\]](#)
58. Chien, C.T.; Li, S.S.; Lai, W.J.; Yeh, Y.C.; Chen, H.A.; Chen, I.S.; Chen, L.C.; Chen, K.H.; Nemoto, T.; Isoda, S.; et al. Tunable Photoluminescence from Graphene Oxide. *Angew. Chem.—Int. Ed.* **2012**, *51*, 6662–6666. [\[CrossRef\]](#)
59. Cedeño, V.J.; Rangel, R.; Cervantes, J.L.; Lara, J.; Alvarado, J.J.; Galván, D.H. Occurrence of Photoluminescence and Onion like Structures Decorating Graphene Oxide with Europium Using Sodium Dodecyl Sulfate Surfactant. *Mater. Res. Express* **2017**, *4*, 075006. [\[CrossRef\]](#)
60. Pashkin, M.O.; Yanykin, D.V.; Popov, A.V.; Pobedonostsev, R.V.; Kazantseva, D.V.; Dorokhov, A.S.; Izmailov, A.Y.; Vyatchinov, A.A.; Orlovskaya, E.O.; Shaidulin, A.T.; et al. Two Types of Europium-Based Photoconversion Covers for Greenhouse Farming with Different Effects on Plants. *Horticulturae* **2023**, *9*, 846. [\[CrossRef\]](#)
61. Walz, H. DUAL-PAM-100 DUAL-PAM/F MANUAL. Available online: <https://www.walz.com/files/downloads/manuals/dual-pam-100/DualPamEd05.pdf> (accessed on 29 September 2023).
62. Yamori, W.; Makino, A.; Shikanai, T. A Physiological Role of Cyclic Electron Transport around Photosystem I in Sustaining Photosynthesis under Fluctuating Light in Rice. *Sci. Rep.* **2016**, *6*, 1–12. [\[CrossRef\]](#) [\[PubMed\]](#)
63. Available online: https://www.walz.com/files/downloads/manuals/gfs-3000/GFS-3000_Manual_9.pdf (accessed on 17 July 2023).
64. Cai, W.; Piner, R.D.; Stadermann, F.J.; Park, S.; Shaibat, M.A.; Ishii, Y.; Yang, D.; Velamakanni, A.; Sung, J.A.; Stoller, M.; et al. Synthesis and Solid-State NMR Structural Characterization of ¹³C-Labeled Graphite Oxide. *Science* **2008**, *321*, 1815–1817. [\[CrossRef\]](#) [\[PubMed\]](#)
65. Novoselov, K.S.; Fal’Ko, V.I.; Colombo, L.; Gellert, P.R.; Schwab, M.G.; Kim, K. A Roadmap for Graphene. *Nature* **2012**, *490*, 192–200. [\[CrossRef\]](#) [\[PubMed\]](#)
66. Wang, X.; Liu, C.; Li, H.; Zhang, H.; Ma, R.; Zhang, Q.; Yang, F.; Liao, Y.C.; Yuan, W.; Chen, F. Metabonomics-Assisted Label-Free Quantitative Proteomic and Transcriptomic Analysis Reveals Novel Insights into the Antifungal Effect of Graphene Oxide for Controlling Fusarium Graminearum. *Environ. Sci. Nano* **2019**, *6*, 3401–3421. [\[CrossRef\]](#)
67. Wang, X.; Xie, H.; Wang, Z.; He, K.; Jing, D. Graphene Oxide as a Multifunctional Synergist of Insecticides against Lepidopteran Insect. *Environ. Sci. Nano* **2019**, *6*, 75–84. [\[CrossRef\]](#)
68. Zhao, G.; Li, J.; Ren, X.; Chen, C.; Wang, X. Few-Layered Graphene Oxide Nanosheets as Superior Sorbents for Heavy Metal Ion Pollution Management. *Environ. Sci. Technol.* **2011**, *45*, 10454–10462. [\[CrossRef\]](#) [\[PubMed\]](#)
69. Zhang, L.; Xia, J.; Zhao, Q.; Liu, L.; Zhang, Z. Functional Graphene Oxide as a Nanocarrier for Controlled Loading and Targeted Delivery of Mixed Anticancer Drugs. *Small* **2010**, *6*, 537–544. [\[CrossRef\]](#)

70. Zhang, M.; Gao, B.; Chen, J.; Li, Y. Effects of Graphene on Seed Germination and Seedling Growth. *J. Nanoparticle Res.* **2015**, *17*, 1–8. [\[CrossRef\]](#)
71. Zhang, X.; Cao, H.; Zhao, J.; Wang, H.; Xing, B.; Chen, Z.; Li, X.; Zhang, J. Graphene Oxide Exhibited Positive Effects on the Growth of *Aloe vera* L. *Physiol. Mol. Biol. Plants* **2021**, *27*, 815–824. [\[CrossRef\]](#)
72. Cheng, F.; Liu, Y.F.; Lu, G.Y.; Zhang, X.K.; Xie, L.L.; Yuan, C.F.; Xu, B.B. Graphene Oxide Modulates Root Growth of *Brassica napus* L. and Regulates ABA and IAA Concentration. *J. Plant Physiol.* **2016**, *193*, 57–63. [\[CrossRef\]](#)
73. Guo, X.; Zhao, J.; Wang, R.; Zhang, H.; Xing, B.; Naeem, M.; Yao, T.; Li, R.; Xu, R.; Zhang, Z.; et al. Effects of Graphene Oxide on Tomato Growth in Different Stages. *Plant Physiol. Biochem.* **2021**, *162*, 447–455. [\[CrossRef\]](#)
74. Zhou, Z.; Li, J.; Li, C.; Guo, Q.; Hou, X.; Zhao, C.; Wang, Y.; Chen, C.; Wang, Q. Effects of Graphene Oxide on the Growth and Photosynthesis of the Emergent Plant *Iris Pseudacorus*. *Plants* **2023**, *12*, 1738. [\[CrossRef\]](#)
75. Perumal, D.; Albert, E.L.; Saad, N.; Hin, T.Y.Y.; Zawawi, R.M.; Teh, H.F.; Che Abdullah, C.A. Fabrication and Characterization of Clinacanthus Nutans Mediated Reduced Graphene Oxide Using a Green Approach. *Crystals* **2022**, *12*, 1539. [\[CrossRef\]](#)
76. Yang, Y.; Zhang, R.; Zhang, X.; Chen, Z.; Wang, H.; Li, P.C.H.; Yang, Y.; Zhang, R.; Zhang, X.; Chen, Z.; et al. Effects of Graphene Oxide on Plant Growth: A Review. *Plants* **2022**, *11*, 2826. [\[CrossRef\]](#) [\[PubMed\]](#)
77. Kiew, S.F.; Kiew, L.V.; Lee, H.B.; Imae, T.; Chung, L.Y. Assessing Biocompatibility of Graphene Oxide-Based Nanocarriers: A Review. *J. Control. Release* **2016**, *226*, 217–228. [\[CrossRef\]](#) [\[PubMed\]](#)
78. Bhattacharya, N.; Cahill, D.M.; Yang, W.; Kochar, M. Graphene as a Nano-Delivery Vehicle in Agriculture—Current Knowledge and Future Prospects. *Crit. Rev. Biotechnol.* **2023**, *43*, 851–869. [\[CrossRef\]](#) [\[PubMed\]](#)
79. Wang, K.; Ruan, J.; Song, H.; Zhang, J.; Wo, Y.; Guo, S.; Cui, D. Biocompatibility of Graphene Oxide. *Nanoscale Res. Lett.* **2011**, *6*, 1–8. [\[CrossRef\]](#) [\[PubMed\]](#)
80. Yigit, O.; Gurgenc, T.; Dikici, B.; Kaseem, M.; Boehlert, C.; Arslan, E. Surface Modification of Pure Mg for Enhanced Biocompatibility and Controlled Biodegradation: A Study on Graphene Oxide (GO)/Strontium Apatite (SrAp) Biocomposite Coatings. *Coatings* **2023**, *13*, 890. [\[CrossRef\]](#)
81. Sun, X.; Liu, Z.; Welsher, K.; Robinson, J.T.; Goodwin, A.; Zaric, S.; Dai, H. Nano-Graphene Oxide for Cellular Imaging and Drug Delivery. *Nano Res.* **2008**, *1*, 203–212. [\[CrossRef\]](#) [\[PubMed\]](#)
82. Wei, W.; Qu, X. Extraordinary Physical Properties of Functionalized Graphene. *Small* **2012**, *8*, 2138–2151. [\[CrossRef\]](#) [\[PubMed\]](#)
83. Li, J.L.; Tang, B.; Yuan, B.; Sun, L.; Wang, X.G. A Review of Optical Imaging and Therapy Using Nanosized Graphene and Graphene Oxide. *Biomaterials* **2013**, *34*, 9519–9534. [\[CrossRef\]](#) [\[PubMed\]](#)
84. Gokus, T.; Nair, R.R.; Bonetti, A.; Böhmmler, M.; Lombardo, A.; Novoselov, K.S.; Geim, A.K.; Ferrari, A.C.; Hartschuh, A. Making Graphene Luminescent by Oxygen Plasma Treatment. *ACS Nano* **2009**, *3*, 3963–3968. [\[CrossRef\]](#) [\[PubMed\]](#)
85. Eda, G.; Lin, Y.Y.; Mattevi, C.; Yamaguchi, H.; Chen, H.A.; Chen, I.S.; Chen, C.W.; Chhowalla, M. Blue Photoluminescence from Chemically Derived Graphene Oxide. *Adv. Mater.* **2010**, *22*, 505–509. [\[CrossRef\]](#)
86. Subrahmanyam, K.S.; Kumar, P.; Nag, A.; Rao, C.N.R. Blue Light Emitting Graphene-Based Materials and Their Use in Generating White Light. *Solid. State Commun.* **2010**, *150*, 1774–1777. [\[CrossRef\]](#)
87. Van Khai, T.; Long, L.N.; Khoi, N.H.T.; Hoc Thang, N. Effects of Hydrothermal Reaction Time on the Structure and Optical Properties of ZnO/Graphene Oxide Nanocomposites. *Crystals* **2022**, *12*, 1825. [\[CrossRef\]](#)
88. Xiao, X.; Zhang, Y.; Zhou, L.; Li, B.; Gu, L. Photoluminescence and Fluorescence Quenching of Graphene Oxide: A Review. *Nanomaterials* **2022**, *12*, 2444. [\[CrossRef\]](#)
89. Xu, B.; Zhu, Y.; Liu, H.; Jin, Z.; Chen, T. The Kinetic and Thermodynamic Adsorption of Eu(III) on Synthetic Maghemite. *J. Mol. Liq.* **2016**, *221*, 171–178. [\[CrossRef\]](#)
90. Ding, C.; Cheng, W.; Sun, Y.; Wang, X. Retracted Article: Determination of Chemical Affinity of Graphene Oxide Nanosheets with Radionuclides Investigated by Macroscopic, Spectroscopic and Modeling Techniques. *Dalton Trans.* **2014**, *43*, 3888–3896. [\[CrossRef\]](#)
91. Qian, Z.S.; Shan, X.Y.; Chai, L.J.; Chen, J.R.; Feng, H. A fluorescent nanosensor based on graphene quantum dots–aptamer probe and graphene oxide platform for detection of lead (II) ion. *Biosens. Bioelectron.* **2015**, *68*, 225–231. [\[CrossRef\]](#)
92. Zhang, S.; Li, Y.; Kang, Y.; Dong, Y.; Hong, S.; Chen, X.; Zhou, J.; Fedoseeva, Y.V.; Asanov, I.P.; Bulusheva, L.G.; et al. Leaky graphene oxide with high quantum yield and dual-wavelength photoluminescence. *Carbon* **2016**, *108*, 461–470. [\[CrossRef\]](#)
93. Mei, Q.; Zhang, K.; Guan, G.; Liu, B.; Wang, S.; Zhang, Z. Highly efficient photoluminescent graphene oxide with tunable surface properties. *Chem. Commun.* **2010**, *46*, 7319–7321. [\[CrossRef\]](#) [\[PubMed\]](#)
94. Jiang, D.; Chen, Y.; Li, N.; Li, W.; Wang, Z.; Zhu, J.; Zhang, H.; Liu, B.; Xu, S. Synthesis of Luminescent Graphene Quantum Dots with High Quantum Yield and Their Toxicity Study. *PLoS ONE* **2015**, *10*, e0144906. [\[CrossRef\]](#) [\[PubMed\]](#)
95. Das, R.C.; Gogoi, K.K.; Das, N.S.; Chowdhury, A. Optimization of quantum yield of highly luminescent graphene oxide quantum dots and their application in resistive memory devices. *Semicond. Sci. Technol.* **2019**, *34*, 125016. [\[CrossRef\]](#)
96. Jafari, H.; Ganjali, M.R.; Shiralizadeh Dezfouli, A.; Kohan, E. A platform for electrochemical sensing of biomolecules based on Europia/reduced graphene oxide nanocomposite. *J. Mater. Sci. Mater. Electron.* **2018**, *29*, 20639–20649. [\[CrossRef\]](#)
97. Lujanienė, G.; Novikau, R.; Joel, E.F.; Karalevičiūtė, K.; Šemčuk, S.; Mažeika, K.; Talaikis, M.; Pakštas, V.; Tumėnas, S.; Mažeika, J.; et al. Preparation of Graphene Oxide-Maghemite-Chitosan Composites for the Adsorption of Europium Ions from Aqueous Solutions. *Molecules* **2022**, *27*, 8035. [\[CrossRef\]](#)

98. Salama, H.M.H.; Al Watban, A.A.; Al-Fughom, A.T. Effect of Ultraviolet Radiation on Chlorophyll, Carotenoid, Protein and Proline Contents of Some Annual Desert Plants. *Saudi J. Biol. Sci.* **2011**, *18*, 79–86. [[CrossRef](#)]
99. Chen, Y.; Li, T.; Yang, Q.; Zhang, Y.; Zou, J.; Bian, Z.; Wen, X. UVA Radiation Is Beneficial for Yield and Quality of Indoor Cultivated Lettuce. *Front. Plant Sci.* **2019**, *10*, 492746. [[CrossRef](#)]
100. McCree, K.J. The Action Spectrum, Absorptance and Quantum Yield of Photosynthesis in Crop Plants. *Agric. Meteorol.* **1971**, *9*, 191–216. [[CrossRef](#)]
101. Wang, S.; Meng, X.; Tang, Z.; Wu, Y.; Xiao, X.; Zhang, G.; Hu, L.; Liu, Z.; Lyu, J.; Yu, J. Red and Blue LED Light Supplementation in the Morning Pre-Activates the Photosynthetic System of Tomato (*Solanum lycopersicum* L.) Leaves and Promotes Plant Growth. *Agronomy* **2022**, *12*, 897. [[CrossRef](#)]

Disclaimer/Publisher’s Note: The statements, opinions and data contained in all publications are solely those of the individual author(s) and contributor(s) and not of MDPI and/or the editor(s). MDPI and/or the editor(s) disclaim responsibility for any injury to people or property resulting from any ideas, methods, instructions or products referred to in the content.